

Structure of Molecular Nitrogen Nanoclusters Containing Stabilized Nitrogen Atoms

C. K. Wetzel¹ · D. M. Lee¹ · V. V. Khmelenko¹

Received: 8 August 2024 / Accepted: 3 October 2024 © The Author(s), under exclusive licence to Springer Science+Business Media, LLC, part of Springer Nature

Abstract

Impurity-helium condensates (IHCs) formed by injecting the discharge products of gaseous mixtures of helium atoms and nitrogen molecules into bulk superfluid 4 He at temperature 1.5 K, were studied by X-band electron spin resonance. IHCs consists of collections of N_2 nanoclusters which form aerogel-like structure inside bulk HeII. It was found that N_2 nanoclusters have a two shell structure, an outer shell which contains high concentration of stabilized N atoms and an interior shell with lower concentrations of N atoms. In this paper, we have studied the dependence of the shell structure of the N_2 nanoclusters which compose the IHCs by varying the ratio of nitrogen to helium in the prepared gas mixture from 0.06 to 1%. The highest local concentration of N atoms in nanoclusters $(1.2 \cdot 10^{21} \, \text{cm}^{-3})$ was observed in the sample prepared from the gas mixture containing the lowest nitrogen admixture (0.06%). Additionally, the evolution of nanocluster structure was studied as the samples were drained of liquid helium $(T \le 3.5 \, \text{K})$ and warmed beyond the point of explosive recombination $(3.5 \, \text{K} \le T \le 6.5 \, \text{K})$.

Keywords Nanoclusters · Matrix isolation · Electron spin resonance

C. K. Wetzel wetzecam@tamu.edu

D. M. Lee dmlee@tamu.edu

V. V. Khmelenko khmel@tamu.edu

Published online: 24 October 2024

Department of Physics and Astronomy, Institute of Quantum Science and Engineering, Texas A&M University, College Station 77843, TX, USA



1 Introduction

The first studies of electron spin resonance (ESR) spectra of nitrogen atoms stabilized in solid molecular matricies were carried out in the middle of the last century [1–7]. The spectroscopic parameters, g-factor, and hyperfine splitting constant, A, for N atoms stabilized in different solid matricies were obtained [4, 6]. Although only small relative concentrations of stabilized N atoms in solid matricies (N/N₂ × 100% \approx 0.1%) were achieved in these studies, it was shown that ESR spectra of stabilized atoms provide important information about their environments in solid matricies. The interaction between nitrogen atoms and their environments increases the hyperfine splitting constant compared to the free atom value [8]. Multiple trapping sites of nitrogen atoms in solid molecular nitrogen were identified [9].

The method of injecting the discharge products of nitrogen-helium gas mixtures into superfluid helium (HeII) allowed for a substantial increase in concentrations of stabilized N atoms [10–12]. Upon entering bulk HeII, the impurity gasses rapidly condense, forming a porous aerogel-like structure composed of nanoclusters containing stabilized atoms. Experiments utilizing x-ray diffraction [13–16] and ultrasound techniques [17-20] have found typical nanocluster sizes ranging from 3 to 6 nm, with pore sizes ranging from 8 to 860 nm. The relative concentrations of nitrogen atoms were found to be 10-30% [21, 22], more than two orders of magnitude larger than that obtained in earlier experiments. It was predicted that most of the stabilized nitrogen atoms should reside on the surfaces of the N₂ nanoclusters [23]. Application of the ESR method for studying the structure of nanoclusters containing stabilized H, D, or N atoms in nanoclusters with different compositions revealed a shell structure of the nanoclusters [24–26]. During condensation of the atoms and molecules with different masses, at the early stage of cooling gas jet, the heavier impurities are freezing first, forming the cores of the nanoclusters due to stronger van der Waals interactions between heavy particles. At the next stage, lighter atoms and molecules stick to the cores of nanoclusters forming the shell structure of the nanoclusters. These nanoclusters form a loosely connected network inside bulk HeII.

The shell structure of nanoclusters composed of nitrogen and different rare gas atoms was extensively studied [27, 28]. In all studied nanoclusters most of the N atoms (70–80%) were stabilized on the nanocluster surfaces. Preliminary studies of N-N₂ nanoclusters were also performed [12, 29]. The highest local concentration of N atoms ($n_{\rm loc} \approx 8 \cdot 10^{20} {\rm cm}^{-3}$) in N₂ nanoclusters immersed into HeII were achieved. The average concentrations of N atoms were of order $n_{\rm avg} \approx 1.4 \cdot 10^{19} {\rm cm}^{-3}$. However, no information about the structure of the N-N₂ nanoclusters, nor the changes of the nanoclusters' structure during warming up were reported.

In this work, we studied N_2 nanoclusters containing stabilized N atoms, prepared from a variety of N_2 -He gas mixtures. The content of N_2 molecules in N_2 -He gas mixtures was varied in the range from 0.0625 to 1%. We found that the N-N₂ nanoclusters possess a two-shell structure for all gas mixtures used. The cores of the nanoclusters consisted of N_2 molecules with small concentration of



stabilized N atoms, and were surrounded by an outer shell with a high concentration of N atoms. It was also found that the average concentration of N atoms stabilized in the collection of N_2 nanoclusters is linear growing with increasing of the quantity of N_2 molecules in the condensed N_2 -He gas mixtures. The local concentrations of N atoms stabilized on the outer shells was found to be largest for the most dilute ($[N_2$:He] = 1:1600) gas mixture. The stability of N atoms in different shells during the process of warming up was also studied.

2 Experimental Setup

The process of forming IHC samples, as well as the experimental setup used in these experiments has been described in great detail elsewhere [28, 30]. Therefore only a brief summary will be provided here. All data presented in this work was gathered using a continuous refill Janis research cryostat, with a base temperature of 1.1 K.

First, a gas mixture of N_2 in ^4He was prepared in a room temperature gas handling system, by diluting spectroscopically pure ^4He (Linde Research Grade Helium Gas) with high purity N_2 (Matheson Research Purity 99.999%). After allowing sufficient time for the gasses to mix (≥ 30 min.), the admixture of gasses were introduced to the cryostat Variable Temperature Insert (VTI), at a constant flux of 3 mL/s ($\frac{dN_2}{dt} = 5 \cdot 10^{19} s^{-1}$), through a liquid nitrogen cooled quartz capillary and RF discharge cavity. Immediately after dissociation, the discharge products exit the quartz capillary through a small orifice (0.75 mm diameter) forming a jet within the VTI. Once in the VTI, the dissociated gas mixture traveled a short distance (≈ 2 cm) before entering a superfluid helium filled quartz beaker. The fast cooling process upon entering the VTI, filled with liquid helium, caused the discharge products to rapidly condense. For each sample studied, this accumulation process was continued for 8 min, before halting the influx of gas mixture and lowering the sample accumulated in the beaker into the ESR cavity located at the bottom of the cryostat.

Upon lowering the sample filled beaker into the ESR cavity the, the X-band microwave bridge was activated and tuned to the cavity resonance frequency of \approx 8.9 GHz. Once tuned and the cryostat allowed to reach its base temperature (typically 1.1 K), ESR registrations of the stabilized nitrogen atoms in the sample as well as a reference ruby signal were taken. The ruby reference signal allowed for calibration of the total number of nitrogen atoms stabilized in the sample [30]. After initial registration and calibration of the ESR signal, of the condensed sample, the VTI was warmed first above the 4 He lambda point, then the beaker drained of liquid helium, while simultaneously recording the atomic nitrogen ESR spectra. Due to the volatility of impurity helium condensates (IHCs) containing high concentrations of atomic nitrogen, registration of the sequences of ESR spectra was unsuccessful for many samples, as explosive recombination of the samples occurred before proper measurements could be taken.

As it was mentioned this set of experiments were carried out in a Janis Research cryostat, with a variable temperature insert volume, connected with a main liquid helium reservoir via a thin capillary. A needle valve at the interface



between the capillary and main helium reservoir allows for regulation of the flux of helium entering the VTI, and a heater located at the interface of the capillary and VTI allows control of the temperature of the helium exiting the orifice. Figure 1 presents a simplified diagram of the experimental setup, emphasizing the temperature control scheme used in these experiments.

A Lakeshore Model 340 temperature control unit was utilized to implement the temperature control feedback loop. The temperature reading from the thermometer embedded in the top of the ESR cavity was used as the feedback point for stabilization. In these experiments, a purely linear proportional, integral, derivative (PID) feedback process was utilized. Due to the physical separation of the heating element and the thermometer used for feedback, a large delay was present in the feedback loop, making the temperature control unstable. Additionally, due to the relatively low thermal conductivity of the quartz beaker and the sample itself, precise measurement of the sample temperature was not possible.

In order to initiate the process of sample destruction and explosion, the needle valve was first closed, and all liquid helium in the VTI evaporated. With no liquid helium remaining in the VTI, the needle valve was partially re-opened and the set point of the temperature controller was set to 3 K, in order to ensure no superfluid helium remained in the VTI. After measurement of the ESR spectra at T=3 K, the temperature controller was set to higher temperatures (5–6.5 K), and registration of the ESR spectra were performed until the explosive destruction of the samples occurred.

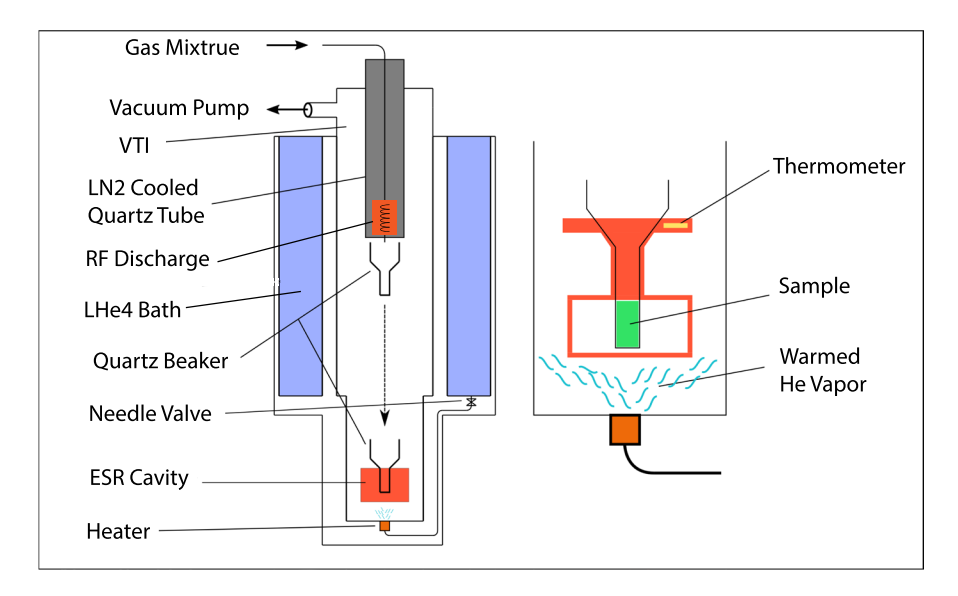


Fig. 1 Simplified diagram of the experimental setup, with emphasis on the temperature control scheme



3 Experimental Results

3.1 Stabilization Efficiency

We studied the dependence of average concentration of N atoms stabilized in $N-N_2$ -He condensates, on the content of N_2 in the initial nitrogen-helium gas mixtures used for sample preparation. The ESR spectra of N atoms, stabilized in N_2 nanoclusters prepared from different nitrogen-helium gas mixtures are shown in Fig. 2. By first measuring the ESR signal of the calibrated ruby crystal located at the bottom of the ESR cavity, then comparing the second integrals of the ruby and nitrogen atoms ESR signals, the average concentration (n_{avg}) of stabilized N atoms was calculated using the following equation.

$$n_{\text{avg}} = \left(N_R \cdot \frac{I_N}{I_R} \cdot \gamma \cdot \frac{4}{3}S(S+1)\right) / V_s \tag{1}$$

where $N_R = 6.417 \cdot 10^{16}$ is the number of spins in the ruby reference crystal, I_N and I_R are the double integrals of the nitrogen ⁴S atoms and ruby signals respectively, $\gamma = 2.66$ is the correction factor for the non-uniform sensitivity of the ESR cavity, $S = \frac{3}{2}$ is the electron spin of a ⁴S ground state ¹⁴N atom, and $V_s = 0.352$ cm³ is the volume of the sample within the cavity. The results of the analysis of ESR spectra are listed in Table 1 and plotted versus nitrogen content in the nitrogen-helium gas mixtures are shown in Fig. 3.

Figure 3 shows almost proportional dependence of average concentration of N atoms stabilized in N_2 nanoclusters, on the amount of N_2 molecules in condensed nitrogen-helium gas mixtures.

Additionally, the efficiency of stabilization of nitrogen atoms (κ) in the samples was calculated as the ratio of the total number of stabilized atoms (N_{tot}) in the sample to the number of atoms sent from the discharge cavity into the superfluid helium filled beaker (N_i), using the following formula,

$$\kappa = \frac{N_{\text{tot}}}{N_i} = \left(n_{\text{avg}} \cdot V_s\right) / \left(\frac{dN_2}{dt} \cdot t_a \cdot \sigma \cdot 2\right)$$
 (2)

where $t_a = 480 \, s$ (8 min) is the accumulation time of the samples, $\frac{dN_2}{dt}$ is the flux of N_2 molecules, and $\sigma \approx 30\%$ is the efficiency of N atom dissociation in discharge. The results of these calculations are listed in Table 1 and plotted versus nitrogen content in the initial gas mixtures, in Fig. 4.

The efficiency of N atoms stabilization initially growing from 0.9 to 3.5% with increasing content of N_2 molecules in the condensed nitrogen-helium gas mixture from 0.06 to 0.25%, but after that it became constant at the level of $\kappa \approx 2.5\%$.



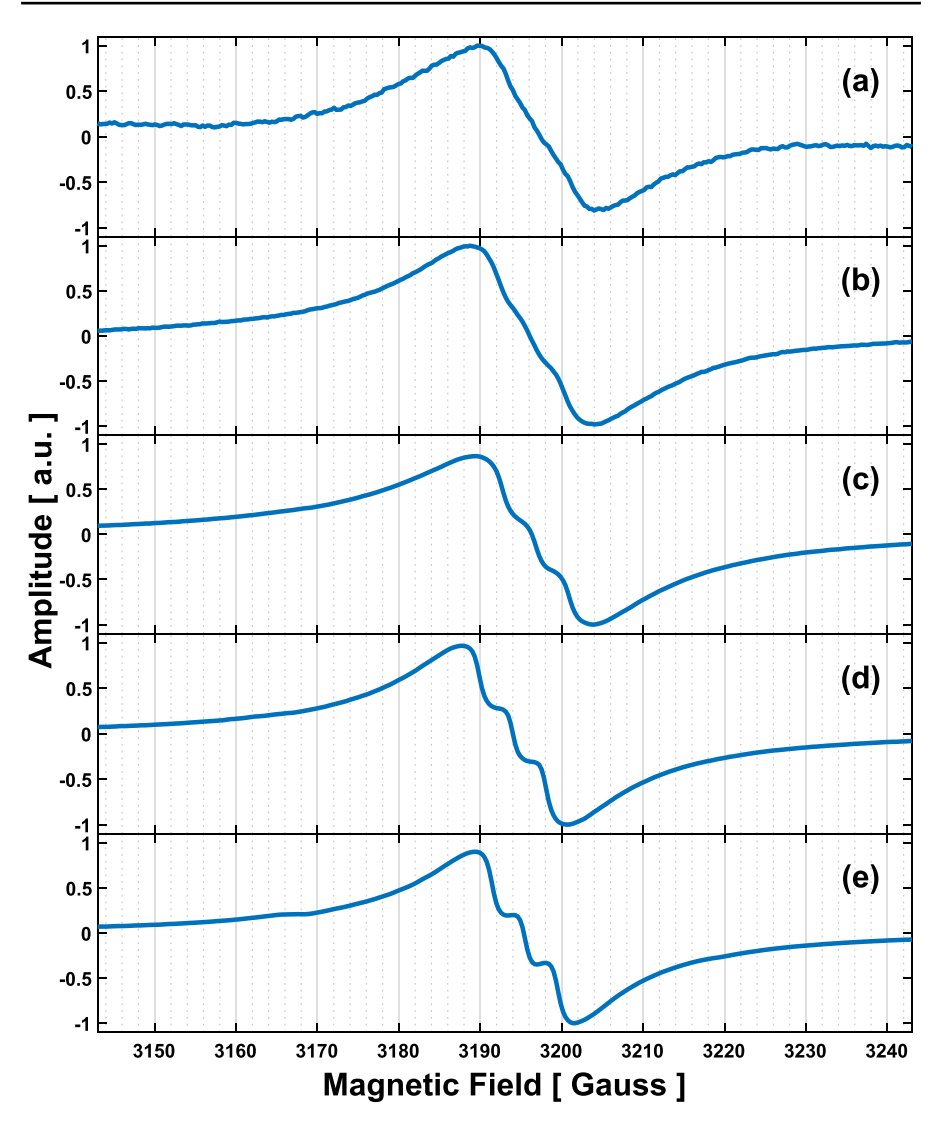


Fig. 2 Derivatives of ESR spectra of N atoms stabilized in the samples prepared from a variety of nitrogen-helium gas mixtures: \mathbf{a} [N_2]:[He] = 1:1600, \mathbf{b} [N_2]:[He] = 1:800, \mathbf{c} [N_2]:[He] = 1:400, \mathbf{d} [N_2]:[He] = 1:200, \mathbf{e} [N_2]:[He] = 1:100. Amplitudes of the spectra were normalized to emphasize the line shape

3.2 Structure of N-N₂ Nanoclusters

Information about the environments of the stabilized nitrogen atoms in N_2 nanoclusters was extracted from the analysis of the line shape of the ESR signals. Previous work on IHC samples [24–28] has established that the constituent N_2 -RG nanoclusters possess a shell structure. The spectroscopic parameters of N atoms stabilized in substitutional sites of N_2 matrix, obtained in previous studies,



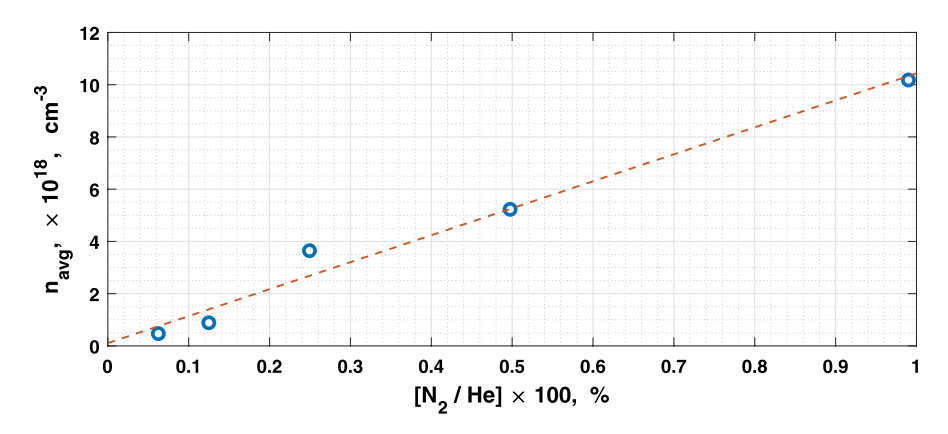


Fig. 3 Dependence of the average concentration of N atoms stabilized in the N-N $_2$ -He samples, on content of N $_2$ in He (%) in the condensed gas mixtures

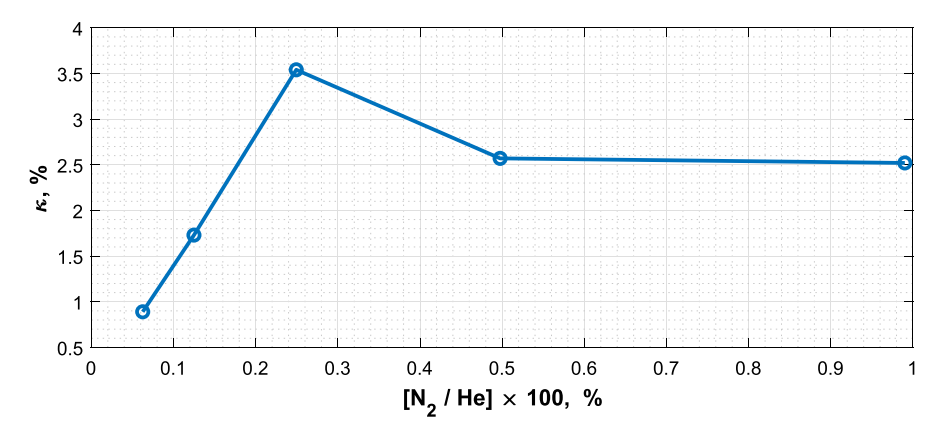


Fig. 4 Dependence of stabilization efficiency of N atoms in the $N-N_2$ -He samples, on the ratio of N_2 /He in the gas mixture used for preparation of samples

Table 1 Flux of nitrogen-helium mixtures used for preparation of IHCs, average concentrations of N(⁴S) atoms within IHCs, and N atom stabilization efficiency

Gas mix- ture [N ₂]:[He]	Flow rate $\frac{dN_2}{dt}$, s ⁻¹	Average concentration n_{avg} , cm ⁻³	N atom stabilization efficiency, κ , %
1:100	4.95×10^{17}	1.02×10^{19}	2.52
1:200	2.49×10^{17}	5.24×10^{18}	2.57
1:400	1.25×10^{17}	3.62×10^{18}	3.54
1:800	6.24×10^{16}	8.82×10^{17}	1.73
1:1600	3.12×10^{16}	2.26×10^{17}	0.89



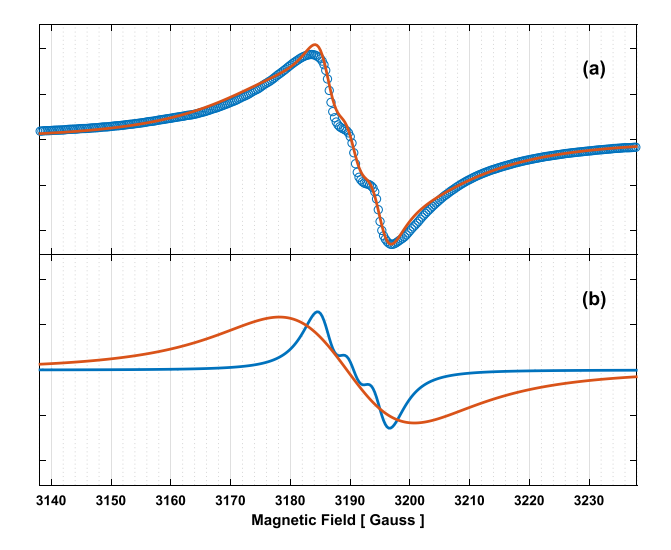


Fig. 5 Derivatives of ESR spectrum of N atoms in nitrogen-helium sample formed by N_2 :He = 1:200 gas mixture: **a** the experimental data (blue circles), and the fit sum of two Lorentzian triplet spectra (solid red line), **b** the two fitting Lorentzian triplets independently, corresponding to the two different environments of N atoms: N atoms on the surfaces (red), N atoms in N_2 matrix (blue) (Color figure online)

Table 2 Hyperfine splitting constants, A and g factors of nitrogen atoms stabilized in substitutional sites in N₂ matrix

Matrix	A, G	g factor
Free [32]	3.73	2.00215
N ₂ [27]	4.20	2.00216
N ₂ [2]	4.31	2.00200(6)
N ₂ [33]	4.22	2.002155(5)
N ₂ [34]	4.21	2.00201(12)

are shown in Table 2. In order to extract information about the N_2 nanoclusters structure the atomic nitrogen ESR signals were modeled as the superposition of two Lorentzian triplets with known hyperfine constants, see Fig. 5. We identified the triplet (blue line) in Fig. 5 with N atoms stabilized in N_2 matrix (A = 4.20 G); and the broad triplet (red line) in Fig. 5 is assigned to N atoms residing on the surfaces of the nanoclusters (A = 4.12 G). The experimental ESR spectra of N atoms were successfully fitted, by using two sets of Lorentzian triplets. The results of analysis are shown in Table 3. This provides evidence for the two shell structure of N_2 nanoclusters formed by injecting nitrogen-helium gas mixtures into bulk HeII. Using the linewidths of the fit spectra components, the local concentrations of the nitrogen atoms residing in each shell were determined using the following formula [31],

$$\Delta H_{\rm pp} = 2.3g\mu_0 \sqrt{S(S+1)} n_{\rm loc} \tag{3}$$



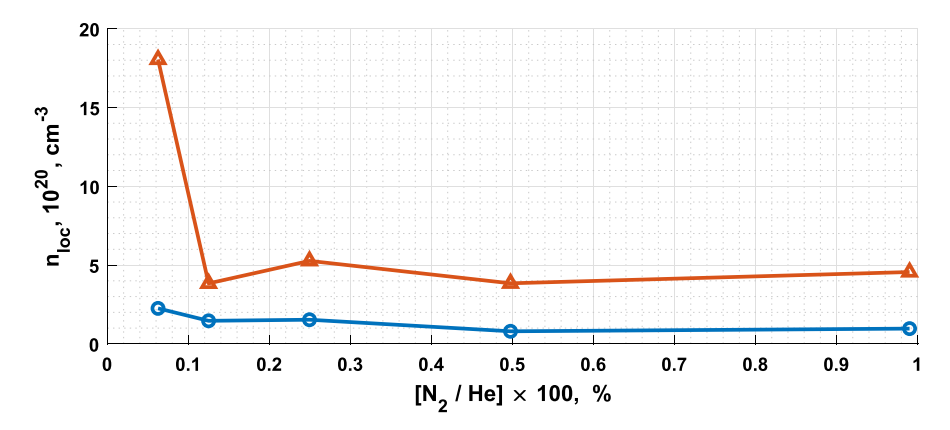


Fig. 6 Dependence of local concentration of N atoms in N_2 nanoclusters, stabilized on nanocluster surfaces (red triangles), and in nanocluster interior cores (blue circles), on the ratio of N_2 (Color figure online)

Table 3 Results from analysis of ESR spectra of N atoms stabilized in molecular nitrogen nanoclusters, prepared from different N_2 :He gas mixtures. Here A is the hyperfine structure constant, g factors of the N atoms and ΔH_{nn} the peak-to-peak linewidth for the derivative ESR spectra

Gas mixture	A, G	$\Delta H_{\rm pp}$, G	$n_{\rm loc}, cm^{-3}$	Weight, %	g factor ¹
[N ₂]:[He] = 1:100	4.12	38.37	4.56×10^{20}	88.20	2.0027
	4.22	8.16	9.67×10^{19}	11.80	2.0020
$[N_2]$:[He] = 1:200	4.12	32.17	3.84×10^{20}	92.20	2.0023
	4.22	6.76	7.97×10^{19}	7.80	2.0023
$[N_2]$:[He] = 1:400	4.12	43.38	5.27×10^{20}	85.65	2.0022
	4.22	12.69	1.53×10^{20}	14.35	2.0030
$[N_2]$:[He] = 1:800	4.12	31.34	3.84×10^{20}	89.69	2.0024
	4.22	11.20	1.46×10^{20}	10.31	2.0021
$[N_2]$:[He] = 1:1600	4.12	102.1	1.80×10^{21}	66.08	2.0015
	4.22	20.82	2.25×10^{20}	33.92	2.0025

¹ The g factor was calculated from the center field H_0 , units G, of the respective triplet and the applied microwave frequency ν , units MHz, using the equation $h\nu = g\mu_0H_0$

where ΔH_{pp} is the peak-to-peak line-width of the ESR derivative line in gauss, g is the electron g-factor, μ_0 is the Bohr magneton, S is the overall electron spin (S=3/2 for ¹⁴N atom), and n_{loc} is the local concentration of nitrogen atoms with units atoms · cm⁻³. Experimental ESR spectra of nitrogen atoms for each as-prepared sample studied has been plotted in Fig. 2, and scaled to unity in order to emphasize the variation in lineshapes. The MATLAB curve fitter application was used to facilitate the fitting of our model to each of the experimental spectra. The results of applying Eq. 3 on the fit spectra are plotted versus nitrogen content of the initial gas mixture in Fig. 6, and also listed in Table 3.



The maximal local concentration of N atoms ($n_{loc}=1.8\cdot 10^{21}\,\mathrm{cm^{-3}}$) was found to be at the surface layer of nanoclusters prepared from gas mixture [N₂:He] = 1:1600. Local concentrations on the surfaces of nanoclusters prepared from less dilute nitrogen-helium gas mixtures were at the level $\approx 5\cdot 10^{20}\,\mathrm{cm^{-3}}$. The local concentrations in the interior layers of nanoclusters for all samples were smaller $\approx (1-2.5)\cdot 10^{20}\,\mathrm{cm^{-3}}$.

3.3 Studies of Changes in N₂ Nanoclusters Structure During Warming up Process

We also studied the changes in the shells of N_2 nanoclusters and total and local concentrations of stabilized atoms during warming up of the collection of nanoclusters prepared from gas mixtures N_2 :He=1:400. In this study, the temperature was incrementally increased over the range 1.1–6.5 K and the ESR spectra of nitrogen atoms were recorded at different temperatures. Figure 7 presents the evolution of N atom ESR spectra as temperature was increased from 3.0 to 6.5 K. In order to obtain information on the structure of N_2 nanoclusters and concentrations of stabilized N atoms, we used the same approach of fitting the experimental ESR spectra as a sum

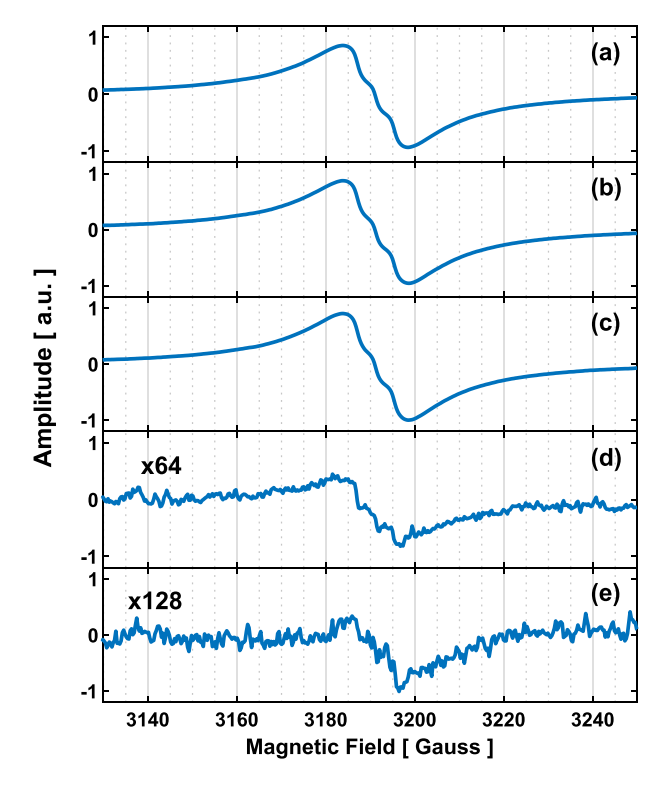


Fig. 7 Derivatives of ESR spectra of N atoms for sample prepared from gas mixture $[N_2]$:[He] = 1:400 at different moments during warming to 5.2 K: **a** 240 s (T = 5.0 K), **b** 260 s (T = 5.0 K), **c** 280 s (T = 4.5 K), **d** 300 s (T = 5.2 K), **e** 320 s (T = 5.2 K). Spectra **d** and **e** were taken after the sample explosion



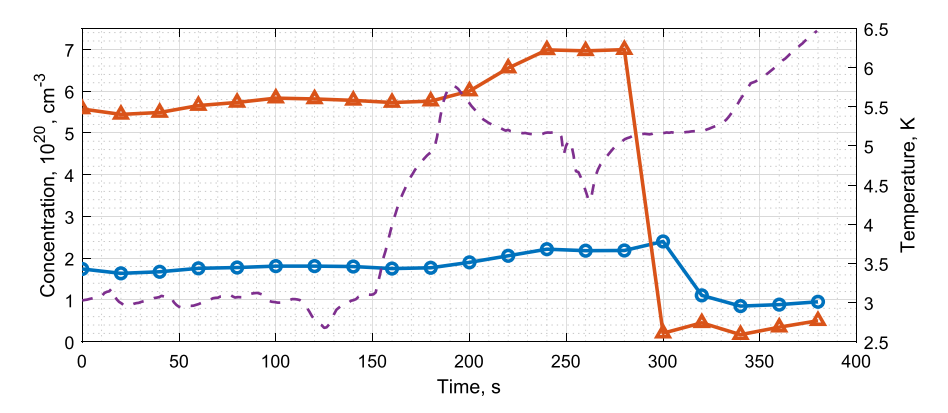


Fig. 8 Time dependence of local concentration of N atoms in N_2 -He nanoclusters, stabilized on nanocluster surfaces (red triangles), and in the cores of N_2 nanoclusters (blue circles), as well as temperature (dashed line) of the ESR cavity during warming from 3-6.5 K. Sample was prepared from gas mixture $[N_2]$: [He] = 1:400 (Color figure online)

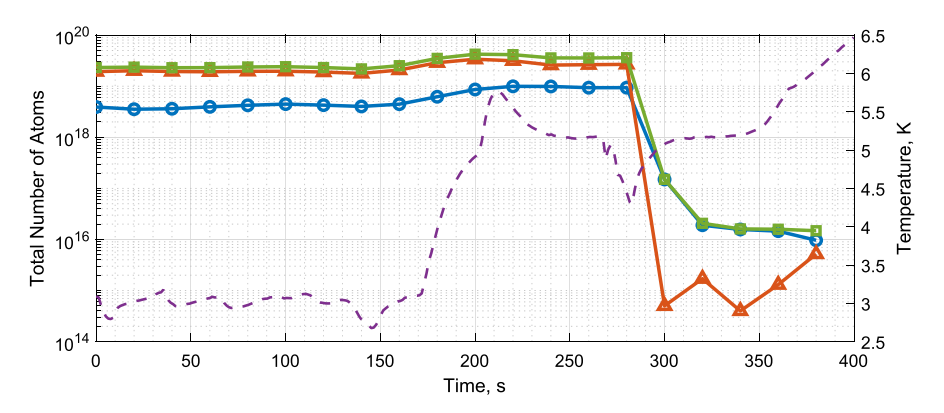


Fig. 9 Time dependence of the total number of N atoms in the sample prepared from gas mixture $[N_2]$: [He] = 1:400 (green squares), and the number of N atoms stabilized on nanocluster surfaces (red triangles), and in the cores of N_2 nanoclusters (blue circles), as well as temperature (dashed line) of the ESR cavity during warming from 3-6.5 K (Color figure online)

of two Lorentzian triplets corresponding to N atoms on the surfaces of nanoclusters and to the N atoms in the N_2 matrix in the interior shell of nanoclusters. From this analysis, we obtained the linewidths and integrals for two sets of fitting Lorentzian triplets, which provided information on local and total concentrations of N atoms stabilized in each of the two shells of N_2 nanoclusters. It was found that N_2 nanoclusters preserved two shell structure in the warm up process even though the local concentrations in each of the shells changed substantially. The time dependences of local concentrations of N atoms on surfaces and in the interior of the N_2 nanoclusters are shown in Fig. 8. The local concentrations in both shells are stable at temperatures below 3.0 K and even have tendency to increase before explosive destruction



of the sample. Sharp reduction of the local concentration of N atoms (\approx 30 times) on the surfaces of nanoclusters occurs at temperature \approx 5.2 K due to chain recombination reactions of N atoms. At the same time, the decrease in the local concentrations in the interior of nanoclusters was much smaller (\approx 2 times).

The time dependence of the total number of N atoms stabilized in the sample, as well as time dependences of the total number of N atoms stabilized on the surfaces and in the interior layers of nanoclusters are shown in Fig. 9. From this figure, one can see that initially most of the N atoms are stabilized on the surfaces of nanoclusters, however, after explosive destruction of the sample most of the survived N atoms are in the interior layers of nanoclusters, their number decreased by a factor of 20. The drop of the total numbers of N atoms on the surfaces is much larger, from 10^{19} to $3 \cdot 10^{14}$ ($3 \cdot 10^4$ times).

4 Discussion

Impurity-helium condensates consist of a collection of nanoclusters, which form aerogel-like structure in superfluid HeII [35]. The size of the nanoclusters (≈ 6 nm) was obtained from x-ray studies [13–16] and the range of pore sizes (8–800 nm) was determined from ultrasound studies [17–19]. These condensates are very promising in achieving high concentrations of stabilized atoms. It was shown that most of the stabilized atoms reside on the surfaces of the nanoclusters. The structure of mixed N_2 -RG and H_2 -RG nanoclusters was extensively studied [24–28]. It was found that nanoclusters have a shell structure. As an example in N_2 -Kr nanoclusters, three shells were identified [24]. The core of nanoclusters was formed by the heaviest krypton atoms, after that the layer of N_2 molecules was formed, and the last outer surface layer was formed. Most of the nitrogen atoms (75–85%) were stabilized on the surfaces of nanoclusters, and only 15–25% were stabilized in the two inner layers. Accordingly the local concentration of atoms stabilized on surfaces of nanoclusters was high, of order $2\cdot 10^{21}\,\mathrm{cm}^{-3}$, an order of magnitude higher than that in the inner layers.

In the previous studies of nitrogen-helium condensates the high average $(10^{19}\,\mathrm{cm^{-3}})$, and local concentration (up to $8\cdot 10^{20}\,\mathrm{cm^{-3}})$ of N atoms were obtained [12, 29]. However, the analysis of the structure of N_2 nanoclusters had not been performed.

In this work, we studied the structure of N_2 nanoclusters in nitrogen-helium condensates formed by condensation of nitrogen-helium gas mixtures, after passing through RF discharge, in bulk HeII. The broad range of ratios of N_2 /He from 1:100 to 1:1600, was used in these experiments. For each samples the ESR spectra of N atom stabilized in N_2 nanoclusters were recorded. From the analysis of the ESR spectra of nitrogen atoms, it was found that the $N-N_2$ nanoclusters have a two shell structure.

The local concentration formula, Eq. 3, assumes Lorentzian broadening due to nearest-neighbor dipole-dipole interactions of irregularly spaced N-atom impurities in the N₂ nanoclusters which constitute the IHC samples. Previous X-ray diffraction studies on IHC samples formed from dilute N₂-He gas mixtures, without discharge



[13, 15], revealed the structure of the N_2 nanoclusters to be hexagonal-icosahedral (hico), with diameter $\sim 60 \text{Å}$. Based on the measured linewidths of the N atom ESR spectra we can calculate the nearest-neighbor separation by $d_{N-N} = (n_{\text{loc}})^{-1/3}$. Taking the averages of the local concentrations for the 4 samples formed from least dilute N_2 -He gas mixtures with similar structure, we estimate the nearest-neighbor distance for N atoms assigned to the surfaces $d_{N-N}^{\text{Surf}} \approx 1.32$ nm, and those assigned to the core $d_{N-N}^{\text{Core}} \approx 2.0$ nm.

In Fig. 10, we present an approximate model for the structure of the N_2 nanoclusters, and distribution of nitrogen atoms stabilized on the nanocluster surfaces. Taking the diameter of an N_2 molecule to be $\approx 3.65 \, \text{Å}$, and knowing the approximate diameter and hico structure of the nanoclusters, we estimate that the average nanocluster contains m=8 icosahedral shells, with a total number of 2057 molecules, and an outer layer of hcp sites on all of the 20 faces, provides 720 possible surface sites, in a fully filled nanocluster.

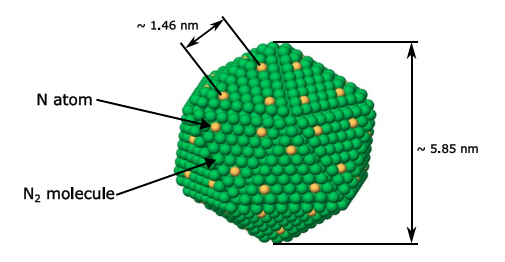
Similar to the case of N_2 -RG nanoclusters, most of the N atoms (70–90%) are stabilized in the outer shells, on the surfaces of nanoclusters, and the rest of the atoms (10–30%) stabilized in N_2 matrix in the interior of the nanoclusters. In the outer (surface) shell, local concentrations of N atoms from $4 \cdot 10^{20}$ cm⁻³ to $1.2 \cdot 10^{21}$ cm⁻³ were achieved. This corresponds to ~ 2 N atom stabilized within the core of each nanocluster, and ~ 40 N atoms stabilized on the surfaces. The local concentrations of N atoms in the inner layer were almost one order of magnitude lower, from $8 \cdot 10^{19}$ cm⁻³ to $2.5 \cdot 10^{20}$ cm⁻³. The average concentrations of stabilized N atoms in the samples were smaller because of the porosity of the samples.

In the samples prepared from nitrogen-helium gas mixtures with different N_2 /He ratios, the average concentration of stabilized N atoms was almost proportional to the content of N_2 molecules in the gas mixture (see Fig. 3).

Figure 11 and Table 4 show comparison of the results obtained in this work and previous [12, 27, 29] studies of average $(n_{\rm avg})$ and local $(n_{\rm loc})$ concentrations of N atoms stabilized in N₂ nanoclusters. In all of these studies, the N-N₂ nanoclusters were formed by injection of the discharge products of nitrogen-helium gas mixtures into bulk superfluid helium.

The largest average N atom concentrations ($\approx 1 \cdot 10^{19}$ were obtained by using gas mixture N₂:He = 1:100. The values of local concentration have tendency to increase

Fig. 10 Idealized model of the $N-N_2$ nanoclusters which constitute the IHC samples of this experiment: green spheres - N_2 molecules, orange spheres - N atoms (Color figure online)





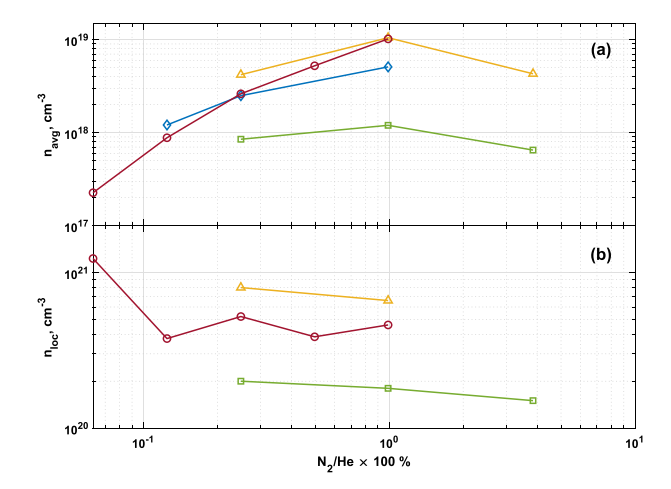


Fig. 11 Dependences of average concentration (a), and local concentration (b) of N atoms stabilized in N_2 nanoclusters on the N_2 /He ratio in nitrogen-helium gas mixtures used for samples preparation obtained in recent work (red circles), from citation [12] (green squares), from citation [27] (blue diamonds), and from citation [29] (yellow triangles) (Color figure online)

Table 4 Comparison of the results for measurements of average (n_{avg}) and local concentrations (n_{loc}) of N atoms stabilized in N₂ nanoclusters obtained in this work (bold) and previous work [12, 27, 29]

2	` '	1
Gas mixture	Average concentration n_{avg} , cm ⁻³	Local concentration n_{loc} , cm ⁻³
$[N_2]$:[He] = 1:25	$4.3 \cdot 10^{18}[29], 6.5 \cdot 10^{17}[12]$	$1.5 \cdot 10^{20}$ [12]
$[N_2]$: $[He] = 1:100$	$5.1 \cdot 10^{18}$ [27], $1.05 \cdot 10^{19}$ [29]	$6.6 \cdot 10^{20}$ [29], $1.8 \cdot 10^{20}$ [12]
	$1.2 \cdot 10^{18}$ [12], 1.02 · 10 ¹⁹	$4.6 \cdot 10^{20}$
$[N_2]$:[He] = 1:200	$5.24 \cdot 10^{18}$	$3.86 \cdot 10^{20}$
$[N_2]$:[He] = 1:400	$2.5 \cdot 10^{18}$ [27], $4.2 \cdot 10^{18}$ [29]	$8 \cdot 10^{20}$ [29], $2 \cdot 10^{20}$ [12]
	$8.5 \cdot 10^{17}$ [12], $2 \cdot 10^{20}$	$5.21 \cdot 10^{20}$
$[N_2]$:[He] = 1:800	$1.21 \cdot 10^{18}$ [27], 8.82 · 10 ¹⁷	$3.76 \cdot 10^{20}$
$[N_2]$:[He] = 1:1600	$2.26 \cdot 10^{17}$	$1.23 \cdot 10^{21}$

The collection of N₂ nanoclusters with stabilized N atoms were formed by injection of nitrogen-helium gas mixtures with different composition into superfluid helium-4

when the admixture of N_2 molecules in nitrogen-helium gas mixtures is decreasing. The maximal local concentration was achieved in this work by using the most dilute gas mixture N_2 :He = 1:1600. It is known that decreasing of N_2 molecules quantity in the nitrogen-helium gas results in reducing sizes of N_2 nanoclusters formed upon injection of gas mixtures into HeII [16]. Therefore, the stabilization of N atoms is more efficient in the nanoclusters with smaller sizes.

Warming of the sample prepared from gas mixtures N_2 :He = 1:400 from 1.1 to 5.0 K does not have an influence on the concentration of N atoms stabilized in different shells of the N_2 nanoclusters. The explosive destruction occurs upon storing



the sample at $T \approx 5.2$ K. After sample destruction, the ESR spectra of the remaining N atoms also can be fitted by two sets of Lorentzian triplets. During the sample explosion the local and total concentrations of N atoms in both shells of N_2 nanoclusters reduced substantially (see Figs. 8 and 9).

5 Conclusion

- 1. The structure of molecular nitrogen nanoclusters containing stabilized N atoms were studied by ESR spectroscopy. The collections of nanoclusters were prepared within superfluid helium, by injection of nitrogen-helium gas mixtures with a broad range of N₂/He ratios in condensed N₂-He gas mixtures. The obtained results provide evidence for two shell structure of N₂ nanoclusters in the samples prepared from gas mixtures with different N₂/He ratios. Most of the N atoms stabilized on the surfaces of N₂ nanoclusters, and much less N atoms stabilized in the interior core of nanoclusters.
- 2. The average concentration of stabilized N atoms in the collections of nanoclusters is proportional to the content of N_2 molecules in the N_2 -He gas mixtures used for samples accumulation. The average concentration of N atoms $n_{avg} = 10^{19}$ was achieved.
- 3. Local concentrations of N atoms stabilized on the surfaces of N_2 nanoclusters on the order of $1.2 \cdot 10^{21}$ cm⁻³ were achieved in this work. These concentrations were obtained in the sample prepared from the most dilute nitrogen-helium gas mixture: $[N_2:He]=1:1600$.
- 4. Behavior of nitrogen atoms in different shells of N_2 nanoclusters were studied as the sample warmed up from 1.1 to 6.5 K. Warming up from 1.1 to 3.0 K did not have an influence on the local concentrations of stabilized N atoms in both shells. Storage of the sample at temperature ≈ 5.2 K led to explosive destruction of nanoclusters, with sharp decrease in N atom concentrations.

Acknowledgements The authors greatly acknowledge the support by the National Science Foundation Grant No. DMR 2104756. CKW acknowledges the support of the HEEP fellowship.

References

- 1. T. Cole, J.T. Harding, J.R. Pellam, D.M. Yost, J. Chem. Phys. 27, 593 (1957)
- 2. S.N. Foner, C.K. Jen, E.L. Cochran, W.A. Bowers, J. Chem. Phys. 28, 351 (1958)
- 3. T. Cole, H.M. McConnel, J. Chem. Phys. 29, 451 (1958)
- 4. C.K. Jen, S.N. Foner, E.L. Cochran, V.A. Bower, Phys. Rev. 112, 1169 (1958)
- 5. L.A. Wall, D.W. Brown, R.E. Florin, J. Chem. Phys. 30, 602 (1959)
- 6. L.A. Wall, D.W. Brown, R.E. Florin, J. Phys. Chem. 63, 1762 (1959)
- 7. S.N. Foner, E.L. Cochran, V.A. Bower, C.K. Jen, J. Chem. Phys. 32, 963 (1960)
- 8. F.J. Adrian, Phys. Rev. **127**, 837 (1962)
- 9. D.D. Delannoy, B. Tribollet, F. Valadier, A. Erbeia, J. Chem. Phys. 68, 2252 (1978)
- 10. E.B. Gordon, L.P. Mezhov-Deglin, O.F. Pugachev, Sov. JETP Lett. 19, 63 (1974)



- E.B. Gordon, A.A. Pelmenev, O.F. Pugachev, V.L. Tal'roze, V.V. Khmelenko, Doklady Phys. Chem. 280(4–6), 145–147 (1985)
- R.E. Boltnev, I.N. Krushinskaya, A.A. Pelmenev, E.A. Popov, D.Yu. Stolyarov, V.V. Khmelenko, Low Temp. Phys. 31, 547 (2005)
- V. Kiryukhin, B. Keimer, R.E. Boltnev, V.V. Khmelenko, E.B. Gordon, Phys. Rev. Lett. 79, 1774 (1997)
- S.I. Kiselev, V.V. Khmelenko, D.M. Lee, V. Kiryukhin, R.E. Boltnev, E.B. Gordon, B. Keimer, Phys. Rev. B 65, 024517 (2002)
- V. Kiryukhin, E.P. Bernard, V.V. Khemelenko, R.E. Boltnev, N.V. Krainyukova, D.M. Lee, Phys. Rev. Lett. 98, 195506 (2007)
- N.V. Krainyukova, R.E. Boltnev, E.P. Bernard, V.V. Khmelenko, V. Kiryukhin, D.M. Lee, Phys. Rev. Lett. 109, 245505 (2012)
- S.I. Kiselev, V.V. Khmelenko, D.A. Geller, D.M. Lee, J.R. Beamish, J. Low Temp. Phys. 119, 357 (2000)
- 18. S.I. Kiselev, V.V. Khmelenko, D.A. Geller, J.R. Beamish, D. Lee, Phys. B 284, 105 (2000)
- 19. S.I. Kiselev, V.V. Khmelenko, D.M. Lee, J. Low Temp. Phys. 121, 671 (2000)
- 20. S.I. Kiselev, V.V. Khmelenko, D.M. Lee, Low Temp. Phys. 26, 641 (2000)
- E.B. Gordon, V.V. Khmelenko, A.E. Popov, A.A. Pelmenev, O.F. Pugachev, Chem. Phys. Lett. 155, 301 (1989)
- E.B. Gordon, A.A. Pelmenev, A.E. Popov, O.F. Pugachev, V.V. Khmelenko, Sov. J. Low Temp. Phys. 15, 48 (1989)
- 23. E.B. Gordon, Low Temp. Phys. **36**, 382 (2010)
- 24. S. Mao, R.E. Boltnev, V.V. Khmelenko, D.M. Lee, Low Temp. Phys. 38, 1037 (2012)
- 25. E.P. Bernard, V.V. Khmelenko, D.M. Lee, J. Low Temp. Phys. **150**, 516–524 (2008)
- R.E. Boltnev, E.P. Bernard, J. Jarvinen, V.V. Khmelenko, D.M. Lee, Phys. Rev. B 79, 180506(R) (2009)
- A. Meraki, P.T. McColgan, R.E. Boltnev, D.M. Lee, V.V. Khmelenko, J. Low Temp. Phys. 192, 224 (2018)
- C.K. Wetzel, D.M. Lee, V.V. Khmelenko, J. Low Temp. Phys. 215, 294–311 (2024). https://doi.org/ 10.1007/s10909-023-03026-5
- 29. E.P. Bernard, R.E. Boltney, V.V. Khmelenko, D.M. Lee, J. Low Temp. Phys. 134, 199 (2004)
- S. Mao, A. Meraki, P.T. McColgan, V. Shemelin, V.V. Khmelenko, D.M. Lee, Rev. Sci. Instrum. 85, 073906 (2014)
- 31. C. Kittel, E. Abrahams, Phys. Rev. 90, 238 (1953)
- 32. M.A. Heald, R. Beringer, Phys. Rev. 96, 645 (1954)
- 33. Yu.A. Dmitriev, R.A. Zhitnikov, Low Temp. Phys. **24**, 44 (1998)
- 34. P.H.H. Fisher, S.W. Charles, C.A. McDonell, J. Chem. Phys. 46, 2162 (1967)
- 35. V.V. Khmelenko, H. Kunttu, D.M. Lee, J. Low Temp. Phys. 148, 1 (2007)

Publisher's Note Springer Nature remains neutral with regard to jurisdictional claims in published maps and institutional affiliations.

Springer Nature or its licensor (e.g. a society or other partner) holds exclusive rights to this article under a publishing agreement with the author(s) or other rightsholder(s); author self-archiving of the accepted manuscript version of this article is solely governed by the terms of such publishing agreement and applicable law.

